

The Casimir frictional drag force between a SiO₂ tip and a graphene-covered SiO₂ substrate

A.I.Volokitin^{1,2*}

¹*Peter Grünberg Institut, Forschungszentrum Jülich, D-52425, Germany and*
²*Samara State Technical University, Physical Department, 443100 Samara, Russia*

The possibility of the mechanical detection of the Casimir friction using the non-contact force microscope is discussed. On a SiO₂ tip situated above a graphene-covered SiO₂ substrate will act the frictional drag force mediated by a fluctuating electromagnetic field produced by a current in the graphene sheet. This friction force will produce the bending of the cantilever, which can be measured by state-of-art non-contact force microscope. Both the thermal and quantum contributions to the Casimir frictional drag force can be studied using this experimental setup. This result paves the ways for the mechanical detection of the Casimir friction and for the application of the frictional drag effect in micro- and nano- electromechanical devices (MEMS and NEMS).

PACS: 42.50.Lc, 12.20.Ds, 78.67.-n

All media are surrounded by a fluctuating electromagnetic field due to the thermal and quantum fluctuations of the current and charge densities inside them. These electromagnetic fluctuations are the cornerstone of the Casimir physics which includes the Casimir – van der Waals forces¹⁻³, the Casimir friction with its limiting case - quantum friction^{3,4}, and the near-field radiative heat transfer^{4,5}. The thermal and quantum fluctuation of the current density in one body induces the current density in other body; the interaction between these current densities is the origin of the Casimir interaction. When two bodies are in relative motion, the induced current will lag slightly behind the fluctuating current inducing it, and this is the origin of the Casimir friction. At present the Casimir friction is attracting a lot of attention due to the fact that it is one of the mechanisms of noncontact friction between bodies in the absence of direct contact⁴. The noncontact friction determines the ultimate limit to which the friction force can be reduced and, consequently, also the force fluctuations because they are linked to friction via the fluctuation-dissipation theorem. The force fluctuations (and hence friction) are important for the ultrasensitive force detection.

The Casimir friction has been studied in the configurations plate-plate^{4,6-10} and neutral particle-plate^{4,11-22}. While the predictions of the theory for the Casimir forces were verified in many experiments³, the detection of the Casimir friction is still challenging problem for experimentalists. However, the frictional drag between quantum wells^{23,24} and graphene sheets^{25,26}, and the current-voltage dependence of nonsuspended graphene on the surface of the polar dielectric SiO₂²⁷, were accurately described using the theory of the Casimir friction²⁸⁻³⁰. In the frictional drag experiment the Casimir friction force between the charge free carriers in the 2D structures mediated by a current density in the one 2D structure induces the electric field in the other 2D structure, which can be measured. For the graphene sheet situated nearby the polar dielectric substrate the Casimir friction force between the charge free carries in graphene and the surface phonon polaritons in dielectric gives rise to the change of the resistivity of graphene which also can be measured. So far the Casimir friction was detected only using the electrical effects, which it produces. Thus, the frictional drag effect can only be observed between the two 2D conducting structures and the electrical transport in graphene can only be measured for nonsuspended graphene when the heat conductance between graphene and underlying dielectric is high.

In this Letter the possibility of the mechanical detection of the Casimir friction using non-contact atomic force microscope (AFM) is considered. The schemes for the experimental setups are shown on Fig.1. On Fig.1a a SiO₂ tip and a SiO₂ substrate have clean surfaces. On Fig.1b a SiO₂ substrate are covered by graphene and a SiO₂ tip has clean surface, and on Fig.1c both surfaces of the tip and the dielectric are covered by graphene. According to the theory of the Casimir friction, the frictional stress between two plates in the parallel relative motion with the velocity v along the \hat{x} -axis and with the \hat{z} -axis normal to the plate is given by the xz -component of the Maxwell stress tensor: $f_{friction} = \sigma_{xz} = f_T + f_0$, where at $d \ll \lambda_T$ and $v \ll c$ the contributions from thermal (f_T) and quantum (f_0) fluctuations are given by^{4,7,10,29}

$$f_T = \frac{\hbar}{\pi^3} \int_0^\infty dq_y \int_0^\infty dq_x q_x e^{-2qd} \left\{ \int_0^\infty d\omega \left(\frac{\text{Im}R_1(\omega)\text{Im}R_2(\omega^+)}{|1 - e^{-2qd}R_1(\omega)R_2(\omega^+)|^2} \times [n_1(\omega) - n_2(\omega^+)] + (1 \leftrightarrow 2) \right) \right\}$$

* Corresponding author. *E-mail address:* alevolokitin@yandex.ru

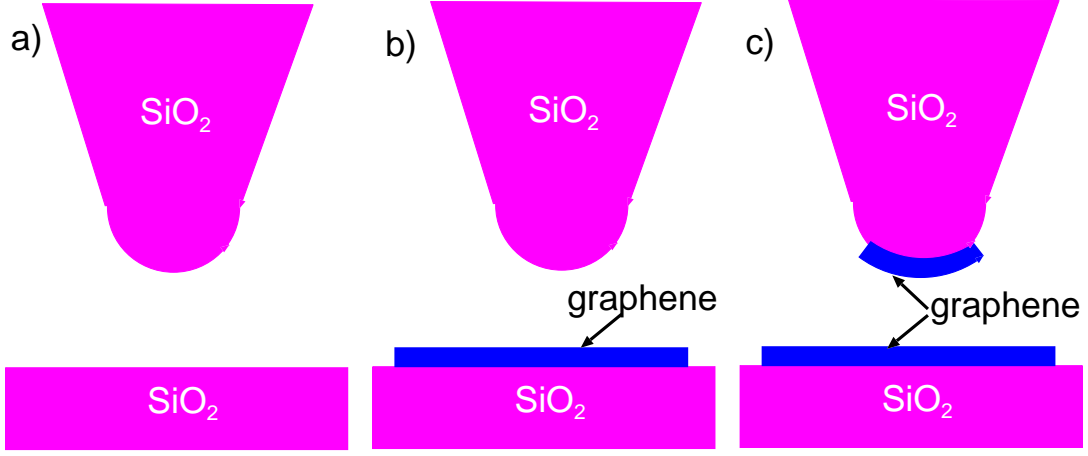


FIG. 1: The different configurations for the observation of the Casimir friction using AFM: a) A SiO₂ tip and a SiO₂ substrate (DD); b) A SiO₂ tip and a graphene- covered SiO₂ substrate (DGD); c) A graphene- covered SiO₂ tip and a graphene- covered SiO₂ substrate (DGGD).

$$- \int_0^{q_x v} d\omega \left(\frac{\text{Im}R_1(\omega)\text{Im}R_2(\omega^-)}{|1 - e^{-2qd}R_1(\omega)R_2(\omega^-)|^2} n_1(\omega) + (1 \leftrightarrow 2) \right) \Bigg\}, \quad (1)$$

$$f_0 = -\frac{\hbar}{2\pi^3} \int_0^\infty dq_y \int_0^\infty dq_x q_x e^{-2qd} \int_0^{q_x v} d\omega \left(\frac{\text{Im}R_1(\omega)\text{Im}R_2(\omega^-)}{|1 - e^{-2qd}R_1(\omega)R_2(\omega^-)|^2} + (1 \leftrightarrow 2) \right). \quad (2)$$

where $\omega^\pm = \omega \pm q_x v$, R_{ip} is the reflection amplitude for the p - polarized electromagnetic wave for the plate i , $n_i(\omega) = [\exp(\omega/k_B T_i) - 1]^{-1}$. The symbol $(1 \leftrightarrow 2)$ denotes the terms that are obtained from the preceding terms by permutation of 1 and 2. The reflection amplitude for the dielectric

$$R_d = \frac{\epsilon_d - 1}{\epsilon_d + 1}, \quad (3)$$

where ϵ_d is the dielectric function for dielectric. The dielectric function of amorphous SiO₂ can be described using an oscillator model³¹

$$\epsilon(\omega) = \epsilon_\infty + \sum_{j=1}^2 \frac{\sigma_j}{\omega_{0,j}^2 - \omega^2 - i\omega\gamma_j}, \quad (4)$$

where parameters $\omega_{0,j}$, γ_j and σ_j were obtained by fitting the actual ϵ for SiO₂ to the above equation, and are given by $\epsilon_\infty = 2.0014$, $\sigma_1 = 4.4767 \times 10^{27} \text{s}^{-2}$, $\omega_{0,1} = 8.6732 \times 10^{13} \text{s}^{-1}$, $\gamma_1 = 3.3026 \times 10^{12} \text{s}^{-1}$, $\sigma_2 = 2.3584 \times 10^{28} \text{s}^{-2}$, $\omega_{0,2} = 2.0219 \times 10^{14} \text{s}^{-1}$, and $\gamma_2 = 8.3983 \times 10^{12} \text{s}^{-1}$. For a graphene-covered SiO₂ substrate the reflection amplitude R_{dg} can be expressed through the reflection amplitudes for the clean substrate surface R_d given by Eq. (3) and for isolated graphene given by²⁸

$$R_g = (\epsilon_g - 1)/\epsilon_g, \quad (5)$$

where the dielectric function of graphene

$$\epsilon_g = 1 + \frac{2\pi i q \sigma_l}{\omega}, \quad (6)$$

where σ_l is the longitudinal conductivity of the sheet. For $qa \ll 1$, where a is the separation between graphene and the dielectric,

$$R_{dg} = 1 - \frac{(1 - R_d)(1 - R_g)}{1 - R_d R_g} = \frac{\epsilon_d - 1 + 2(\epsilon_g - 1)}{\epsilon_d + 1 + 2(\epsilon_g - 1)}. \quad (7)$$

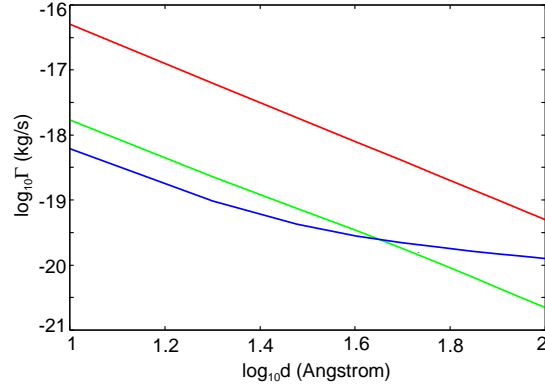


FIG. 2: The dependence of the friction coefficient Γ for the spherical tip with the radius of the curvature $R = 1\mu\text{m}$ on the separation d between the tip and the substrate for the different configurations at $T = 300\text{K}$. The red, green and blue curves represent the results for the configurations (a) DD (Fig.1a), (b) DGD (Fig.1b), and (c) DGGD (Fig.1c), respectively. The charge carriers concentration for graphene $n = 10^{16}\text{m}^{-2}$

In the study below we used the dielectric function of graphene, which was calculated within the random-phase approximation (RPA)^{32,33}. The dielectric function is an analytical function in the upper half-space of the complex ω -plane:

$$\varepsilon_0(\omega, q) = 1 + \frac{4k_F e^2}{\hbar v_F q} - \frac{e^2 q}{2\hbar \sqrt{\omega^2 - v_F^2 q^2}} \left\{ G\left(\frac{\omega + 2v_F k_F}{v_F q}\right) - G\left(\frac{\omega - 2v_F k_F}{v_F q}\right) - i\pi \right\}, \quad (8)$$

where

$$G(x) = x\sqrt{x^2 - 1} - \ln(x + \sqrt{x^2 - 1}), \quad (9)$$

where the Fermi wave vector $k_F = (\pi n)^{1/2}$, n is the concentration of charge carriers, the Fermi energy $\epsilon_F = \hbar v_F k_F$, $v_F \approx 10^6$ m/s is the Fermi velocity.

An atomic force microscope tip with the radius of curvature $R \gg d$, at a distance d above a flat sample surface, can be approximated by a sphere with radius R . In this case the friction force between the tip and the plane surface can be estimated using the approximate method of Derjaguin³⁴, later called the proximity force approximation (PFA)³⁵. According to this method, the friction force in the gap between two smooth curved surfaces at short separation can be calculated approximately as a sum of forces between pairs of small parallel plates corresponding to the curved geometry of the gap. Specifically, the sphere-plane friction force is given by

$$F_{friction} = 2\pi \int_0^R d\rho \rho f_{friction}(z(\rho)), \quad (10)$$

where $z(\rho) = d + R - \sqrt{R^2 - \rho^2}$ denotes the tip-surface distance as a function of the distance ρ from the tip symmetry axis, and the friction force per unit area $f_{friction}(z(\rho))$ is determined for flat surfaces.

To linear order in the velocity v the friction force $f_{friction} = \gamma v$ where at $T_1 = T_2 = T$ the friction coefficient

$$\gamma = \frac{\hbar^2}{8\pi^2 k_B T} \int_0^\infty \frac{d\omega}{\sinh^2\left(\frac{\hbar\omega}{k_B T}\right)} \int_0^\infty dq q^3 e^{-2qd} \frac{\text{Im}R_{1p}\text{Im}R_{2p}}{|1 - e^{-2qd}R_{1p}R_{2p}|^2}. \quad (11)$$

The friction coefficient in the tip-plane configuration Γ can be obtained from Eq.(11) using the proximity force approximation. In an experiment Γ is determined by measuring the quality factor of the cantilever vibration parallel to the substrate surface³⁶. At present can only be detected the friction coefficient in the range $10^{-12} - 10^{-13}\text{kg/s}$ ³⁶. Fig.2 shows the dependence of the friction coefficient on the separation between a tip and a substrate surface for the different configurations. The red, green and blue curves represent the results for the configurations (a) $\text{SiO}_2\text{-SiO}_2$ (DD) (Fig.1a), (b) $\text{SiO}_2\text{+graphene-SiO}_2$ (DGD) (Fig.1b), and (c) $\text{SiO}_2\text{+graphene - SiO}_2\text{+graphene}$ (DGGD) (Fig.1c), respectively. The friction coefficient in these configurations is below 10^{-16}kg/s thus it can not be tested by the modern experimental setup. However, it has been predicted in Ref.³⁷, that for the some configurations involving adsorbates the Casimir friction coefficient can be large enough to be measured by state-of-art non-contact force microscope.

During the cantilever vibration the velocity of the AFM tip does not exceed 1m/s. However, the Casimir friction force can be strongly enhanced at the large relative sliding velocity. This friction force can be detected if it produces sufficiently large bending of the cantilever. Fig. 3 shows the dependence of the friction force, acting on the tip with the radius of the curvature $R = 1\mu\text{m}$, on the relative velocity v between the tip and substrate for the SiO₂-SiO₂ configuration (see Fig.1a) at the separation $d = 1\text{nm}$ and for the different temperatures. The friction force $F_{friction} = F_0 + F_T$ where F_0 is the contribution from quantum fluctuations which exist even at $T = 0\text{K}$ (this friction is denoted as quantum friction⁶, $F_{friction}(T = 0\text{K}) = F_0$) and F_T is the contribution from the thermal fluctuations which exist only at finite temperature. The thermal contribution dominates for $v < k_B T d / \hbar$ and quantum contribution dominates for $v > k_B T d / \hbar$. On Fig.3 $F_{friction} > 10^{-12}\text{N}$ at $v > 10^5$. In the modern experiment³⁸ the spring constant of the cantilever are between $k_0 = 30$ and $k_0 = 50\mu\text{N/m}$. The friction force $\approx 10^{-12}\text{N}$ will produce the displacement of the tip of the order 10^2nm which can be easily detected. However, at present there is no experimental setup with the relative sliding velocity between the tip and substrate $\sim 10^5\text{m/s}$.

An alternative method for the detection of the Casimir friction is possible for the SiO₂+graphene - SiO₂ configuration (see Fig.1b). For this configuration inducing current in a graphene sheet with the drift velocity v_{Drift} will produce the fluctuating electromagnetic field which is similar to the electromagnetic field due to the mechanical motion of the sheet with the velocity $v = v_{Drift}$ ^{4,28-30}. Due to the high mobility of the charge carriers in graphene, in a high electric field electrons (or holes) can move with very high velocities (up to 10^6 m/s). The drift motion of charge carries in graphene will result in a modification of dielectric properties of graphene due to the Doppler effect⁶. The reflection amplitude for the graphene sheet with induced current density is determined by the reflection amplitude R'_g in the reference frame co-moving with the drift motion of the charge carriers in graphene: $R'_g = R_g(\omega^-)$, where $R_g(\omega)$ is the reflection amplitude amplitude in the rest reference frame of graphene in the equilibrium state, $\omega^- = \omega - q_x v$, $v = v_{Drift}$.

In the vacuum gap between two plates in the configuration SiO₂+graphene - SiO₂ the electric field $\mathbf{E}(\mathbf{q}, \omega, z)$ can be written in the form¹⁰

$$\mathbf{E}(\mathbf{q}, \omega, z) = v_p \hat{n}_p^+ e^{-qz} + w_p \hat{n}_p^- e^{qz}, \quad (12)$$

where $\hat{n}_p^\pm = (\mp i\mathbf{q}, q)$,

$$v_p = \frac{E_{dg}^{f'} + R'_{dg} E_d^f e^{-qd}}{1 - e^{-2qd} R'_{dg} R_d}, \quad w_p = \frac{R_d E_{dg}^{f'} e^{-2qd} + E_d^f e^{-qd}}{1 - e^{-2qd} R'_{dg} R_d}, \quad (13)$$

where $E_{dg}^{f'}$ and E_d are the amplitudes of the fluctuating electric fields created in vacuum on the surfaces of the plates SiO₂+graphene and SiO₂ by the charge density fluctuations inside the plates SiO₂+graphene and SiO₂, respectively, and where, in the presence of the induced current density in a graphene sheet with the drift velocity v_{Drift} , the reflection amplitude R'_{dg} is given by Eq.(7) with R_g replaced on $R'_g = R_g(\omega^-)$

$$R'_{dg} = 1 - \frac{(1 - R_d)(1 - R'_g)}{1 - R_d R'_g} = \frac{\epsilon_d - 1 + 2(\epsilon'_g - 1)}{\epsilon_d + 1 + 2(\epsilon'_g - 1)}, \quad (14)$$

where $\epsilon'_g = \epsilon_g(\omega^-)$. The electric field $E_{dg}^{f'}$ is resulting from the interference of the electric fields created by the SiO₂ plate and the graphene sheet at $qa \ll 1$ is given by

$$E_{dg}^{f'} = \frac{E_d^f(1 - R'_g) - 2E_g^{f'}(1 - R_d)}{1 - R_d R'_g} = \frac{E_d^f(\epsilon_d + 1) - 2E_g^{f'}\epsilon'_g}{\epsilon_d + 1 + 2(\epsilon'_g - 1)}, \quad (15)$$

where E_d^f and R'_g are the electric fields created by the SiO₂ plate and by the graphene sheet with the drift motion of the charge carriers on the surface of the SiO₂+graphene plate, respectively. According to the general theory of the fluctuating electromagnetic field⁴ the spectral density of the fluctuations for the electric field :

$$\langle |E_i^f|^2 \rangle_\omega = \frac{2\hbar}{q} \left(n_i(\omega) + \frac{1}{2} \right) \text{Im} R_i, \quad (16)$$

where $\langle \dots \rangle$ denote statistical average over the random field, $i = d, g$. The frictional stress f_x acting on the surface of the SiO₂ plate is determined by xz -component of Maxwell's stress tensor σ_{ij} , calculated at $z = +0$:

$$f_x = \sigma_{xz} = \frac{1}{8\pi} \int_{-\infty}^{+\infty} d\omega [\langle E_z E_x^* \rangle + \langle E_z^* E_x \rangle]_{z=+0} = 2\text{Im} \int_0^\infty \frac{d\omega}{2\pi} \int \frac{d^2q}{(2\pi)^2} \frac{q_x}{q} \langle w_p^* v_p \rangle, \quad (17)$$

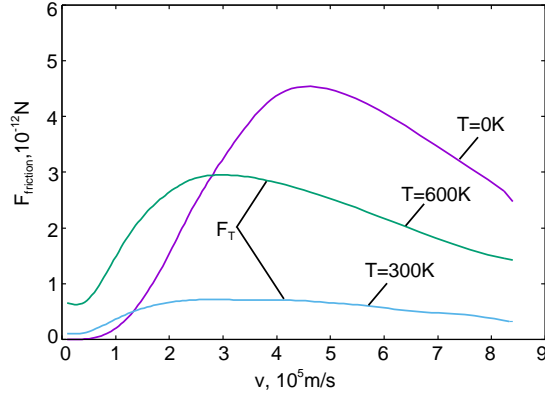


FIG. 3: The dependence of the friction force $F_{friction} = F_0 + F_T$ acting on the spherical tip with the radius of the curvature $R = 1\mu\text{m}$ on the relative sliding velocity v between the tip and the substrate for the $\text{SiO}_2\text{-SiO}_2$ configuration (see Fig. 1a) at the separation $d = 1\text{nm}$ and for the different temperatures, where F_0 is the contribution to the friction force due to the quantum fluctuations (this friction is denoted as quantum friction⁶, $F_{friction}(T = 0\text{K}) = F_0$) and F_T is the thermal contribution from the thermal fluctuations.

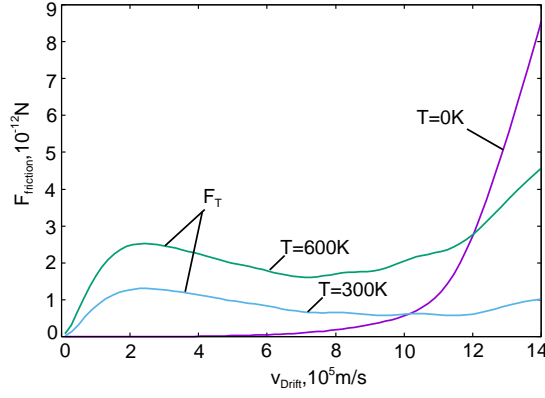


FIG. 4: The same as on Fig. 3 but for the dependence of the friction force on the drift velocity v_{Drift} of the charge carriers in graphene for the $\text{SiO}_2\text{+graphene-SiO}_2$ configuration (see Fig. 1b).

where the symbol $\langle \dots \rangle$ denotes statistical averaging on the random fields \mathbf{E}_d^f and \mathbf{E}_g^f . Using Eqs. (12)-(15) in Eq.(17), after averaging over the random electric fields in Eq.(17) using Eq.(16), we get

$$f_x = \frac{\hbar}{2\pi^3} \int_0^\infty d\omega \int d^2q q_x \frac{\text{Im}R_d}{|1 - e^{-2qd}\text{Im}R_d\text{Im}R'_{dg}|^2} \left(\text{Im}R'_{dg}[n_g(\omega^-) - n_d(\omega)] \right. \\ \left. + \frac{2\text{Im}\epsilon_d}{|\epsilon_d + 1 + 2(\epsilon_g^- - 1)|^2} [n_g(\omega) - n_g(\omega^-)] \right). \quad (18)$$

In Eq. (18) the arguments T_g and T_d in the factors n_g and n_d are the temperatures of the $\text{SiO}_2\text{+graphene}$ and SiO_2 plates, respectively. The contribution to the friction from the quantum fluctuations can be obtained from Eq. (18) at $T_g = T_d = 0\text{K}$

$$f_x(T = 0\text{K}) = -\frac{2\hbar}{\pi^3} \int_0^\infty d\omega \int d^2q q_x \frac{\text{Im}R_d\text{Im}\epsilon'_g}{|1 - e^{-2qd}\text{Im}R_d\text{Im}R'_{dg}|^2 |\epsilon_d + 1 + 2(\epsilon'_g - 1)|^2} \quad (19)$$

Fig.4 shows the dependence of the frictional drag force acting on the SiO_2 tip in the $\text{SiO}_2\text{+graphene-SiO}_2$ configuration on the drift velocity v_{Drift} of electrons in the graphene sheet. For $v_{Drift} > 10^5\text{m/s}$ the friction force is above 10^{-12}N and can be measured by state-of-art non-contact force microscope. The contribution to the friction force from

the thermal fluctuations dominates at $v_{Drift} < 10^6$ m/s and the contribution from quantum fluctuations dominates for $v_{Drift} > 10^6$ m/s. It is important to note that in the contrast to the SiO₂-SiO₂ configuration, where the bending of the cantilever due to the Casimir friction can only be detected for very large relative sliding velocity between a tip and a substrate, in the SiO₂+graphene-SiO₂ configuration the friction of the same order can be obtained inducing the current density in the graphene sheet.

Conclusion A current in the graphene sheet produces a fluctuating electromagnetic field which is similar to the field produced by the moving sheet. In a high electric field electrons in non suspended graphene on the SiO₂ substrate can move with sufficiently large drift velocity (above 10^6 m/s²⁷) to produce the frictional drag force acting on a tip which can be measured by state-of-art non-contact force microscope. Both the thermal and quantum contributions to the Casimir friction can be detected using this experimental setup. These results pave the ways for the mechanical detection of the Casimir friction and for the application of the frictional drag effect in micro- and nano- electromechanical devices (MEMS and NEMS).

The study was supported by the Russian Foundation for Basic Research (Grant No. 16-02-00059-a).

-
- ¹ H.B.G. Casimir, Proc. K. Ned. Akad. Wet. **51**, 793 (1948).
² E.M. Lifshitz, Zh. Eksp. Teor. Fiz. **29**, 94 (1955) [Engl. Trnsl. 1956 Sov. Phys.-JETP **2**, 73 (1956)].
³ *Casimir Physics*. Ed. by D.A.R. Dalvit, P. Milonni, D. Roberts and F. da Rose (Springer, Berlin 2011).
⁴ A.I. Volokitin and B.N.J. Persson, Rev.Mod.Phys. **79**, 1291 (2007).
⁵ D.Polder and M.Van Hove, Phys. Rev. B **4**, 3303, (1971).
⁶ J.B. Pendry, J. Phys.: Condens.Matter **9**, 10301 (1997).
⁷ A.I. Volokitin and B.N.J. Persson, J. Phys.: Condens.Matter **11**, 345 (1999).
⁸ A. I. Volokitin and B. N. J. Persson, Phys. Rev. Lett. **91**, 106101 (2003).
⁹ A. I. Volokitin and B. N. J. Persson, Phys. Rev. B, **68**, 155420 (2003).
¹⁰ A.I. Volokitin and B.N.J. Persson, Phys. Rev. B **78**, 155437 (2008).
¹¹ M. S. Tomassone and A. Widom, Phys. Rev. B **56**, 4938 (1997)
¹² A. I. Volokitin and B. N. J. Persson, Phys. Rev. B **65**, 115419 (2002)
¹³ G. V. Dedkov and A. A. Kyasov, Phys. Lett. A **339**, 212 (2005).
¹⁴ G. V. Dedkov and A. A. Kyasov, *J.Phys.:Condens.Matter* **20**, 354006 (2008).
¹⁵ G. Barton, New J. Phys. **12**, 113045 (2010).
¹⁶ J. S. Høye and I. Brevik, Entropy **15**, 3045 (2013).
¹⁷ J. S. Høye and I. Brevik, Eur. Phys. J. D **68**, 61 (2014).
¹⁸ M. F. Maghrebi, R. Golestanian and M. Kardar, Phys. Rev. D **87**, 025016 (2013).
¹⁹ F. Intravaia, R. O. Behunin and D. A. R. Dalvit, Phys. Rev. A **89**, 050101(R) (2014).
²⁰ A.I. Volokitin and B.N.J. Persson, New J. Phys. **16**, 118001 (2014).
²¹ G. Pieplow and C. Henkel, New J. Phys. **15**, 023027 (2013).
²² G. Pieplow and C. Henkel, J. Phys.: Condens. Matter **27**, 214001 (2015).
²³ T.J. Gramila, J.P. Eisenstein, A.H. MacDonald, L.N. Pfeiffer, and K. W. West, Phys. Rev. Lett. **66**, 1216 (1991).
²⁴ U. Sivan, P.M. Solomon, and H. Shtrikman, Phys. Rev. Lett. **68**, 1196 (1992).
²⁵ S.Kim, I.Jo, J.Nah, Z.Yao, S.K.Banerjee and E.Tutuc, Phys. Rev. B **83** 161401 (2011).
²⁶ R.V.Gorbachev, A.K.Geim, M.I.Katsnelson, K.S.Novoselov, T.Tudorovskiy, T.V.Grigorieva, A.H.MacDonald, K.Watanabe, T.Taniguchi and L.P.Ponamarenko Nature Phys. **8** 896 (2012).
²⁷ M. Freitag, M. Steiner, Y. Martin, V. Perebeinos, Z. Chen, J.C. Tsang, and P. Avouris, Nano Lett. **9**, 1883 (2009).
²⁸ A.I.Volokitin and B.N.J. Persson, J.Phys.: Condens. Matter **13**, 859 (2001).
²⁹ A.I. Volokitin and B.N.J. Persson, Phys. Rev. Lett. **106**, 094502 (2011).
³⁰ A.I.Volokitin and B.N.J. Persson, EPL **103**, 24002(2013).
³¹ D.Z.A. Chen, R. Hamam, M. Soljacic, J.D. Joannopoulos and G. Chen, Appl. Phys. Lett. **90**, 181921 (2007).
³² B. Wunscvh, T. Stauber, F. Sols, and F. Guinea, New J.Phys. **8**,318 (2006).
³³ E.H. Hwang, S.Das Sarma, Phys. Rev. B **75**, 205418 (2007).
³⁴ B. Derjaguin, Kolloid-Z. **69**, 155 (1934).
³⁵ Blocki, J., J. Randrup, W. J. Swiatecki, and C. F. Tsang, Ann.Phys. (N.Y) **105**, 427 (1977).
³⁶ E. Gnecco and E. Meyer, *Elements of friction theory and nanotribology*, ed. by E. Gnecco and E. Meyer (Cambridge University Press 2015).
³⁷ A. I. Volokitin and B. N. J. Persson, and H. Ueba, Phys. Rev. B **73**, 165423 (2006).
³⁸ A. Mehlin, F. Xue, D. Liang, H. F. Du, M. J. Stolt, S. Jin, M. L. Tian, and M. Poggio, Nano Lett. **15**, 4839 (2015).